UDC 544:544.6:541.13:541.183:541.138

V. Knysh, O. Shmychkova, T. Luk'yanenko, A. Velichenko

TEMPLATE SYNTHESIS FOR THE CREATION OF PHOTO- AND ELECTROCATALYSTS

Ukrainian State University of Chemical Technology, Dnipro, Ukraine

This work reports the optimal conditions for the synthesis of a matrix for the creation of photo- and electrocatalysts. Specifically, it is shown that TiO_2 nanotube arrays has a high specific surface area and improved catalytic properties, but has low conductivity and weak structural strength, that requires further optimization. The original TiO_2 nanotubes were prepared by anodizing of Ti foil in ethylene glycol with 0.3 wt.% ammonium fluoride and 2 vol.% water at a constant potential, followed by another anodizing in ethylene glycol with 5 wt.% H_3PO_4. The reduction was conducted in 1 M $HClO_4$. Some samples were thermally treated in the air using tube furnace. The study demonstrates how the synthesis conditions of the coating affect the morphology and stoichiometry of the resulting oxide coating. For the obtained materials, the Tafel slope in the oxygen evolution reaction is determined by the semiconductor characteristics of the coating, which, in turn, depend on the stoichiometry of the synthesized oxide. The higher the stoichiometry in the oxygen sublattice, the fewer the charge carriers and the greater the contribution of the semiconductor component to the Tafel slope. As for hydrogen evolution, the layers obtained after heat treatment show a lower Tafel slope (175 mV dec^{-1}).

Keywords: titanium nanotube arrays, inner layer, semiconductor properties, electrodeposition, oxygen evolution reaction, hydrogen evolution reaction.

DOI: 10.32434/0321-4095-2023-148-3-86-93

Introduction

The development of methods for electrochemical formation of catalytically active systems is one of the important tasks of modern electrochemistry, as existing methods for obtaining catalysts are labor-intensive and technologically complex [1]. Applying a catalytic coating to a substrate aims to increase the strength of the catalyst, as well as its resistance to thermal and mechanical stress. Among the known methods for applying a catalytically active layer, the electrochemical method stands out, which allows forming coatings of the required composition and thickness, ensuring high adhesion and significantly reducing the manufacturing time of the catalyst by excluding additional stages [2]. Issues of improving the technology of applying catalytically active coatings with platinum group metals, including on substrates of non-noble metals and alloys, forming their highly developed surface, and a rational choice of electrolytes to control the composition of the composite, are undoubtedly relevant, and solving these problems is impossible without improving existing and developing new methods for the coating synthesis.

At the same time, considering the scarcity and high cost of platinum group metals, great attention is paid to reducing the content of noble metals in catalytically active systems. The rational choice of the catalyst composition allows the coating to provide the necessary thermal stability, reduce the transition resistance, and increase its corrosion resistance. Recently, the scope of application of metallic carriers for catalytic coatings has been expanding, which are distinguished by high mechanical strength, plasticity, thermal conductivity, improving thermal regulation and preventing catalyst overheating compared to ceramic carriers. However, the main disadvantage of a metallic carrier is its low specific surface area, which can be increased by anodic treatment [3].

The preliminary treatment of the substrate surface is of significant importance in creating systems that are operational in a wide range of conditions. One of the most effective methods for preparing the surface is the electrochemical method [1–3].

The electrode material plays a crucial role in the electrochemical process for effective removal of organic pollutants. Over the past two decades, the metal oxide electrode (SnO_2, Sb-doped SnO_2, PbO_2, IrO_2, etc.) with Ti as a substrate has been widely used for wastewater treatment [4,5]. Although the traditional SnO_2 or doped SnO_2 electrodes have excellent catalytic properties and high oxygen evolution potential [6], their low electrode stability limit further application. Compared with the doped SnO_2 electrode, the PbO_2 electrode has a longer service life with stable electrochemical properties but has low electrocatalytic activity [7]. Recently, a TiO_2 nanotube array (NTA) has emerged, which has been reported to improve electrode properties [8–10], as TiO_2 NTA has a highly ordered vertical array structure with a high specific surface area. TiO_2 NTA is usually fabricated as an inner layer to enhance the stability and catalytic properties of electrodes [11].

In this work, we selected the optimal synthesis conditions for the template to create photo- and electrocatalysts. The internal layer should meet several requirements, including (i) high electrical conductivity to enable electrochemical deposition of the metal; and (ii) the material should possess a high number of charge carriers, which can include semiconductors with a high number of charge carriers.

However, TiO_2 NTA is a coating obtained by typical anodizing method, which has some defects such as low conductivity and weak structural strength [11]. Here, the preparation process still requires further improvement to optimize material stability. In some previous studies [12], a reinforced TiO_2 NTA anode was developed by double anodization and cathodization to remove the fluoride-rich TiO_2 layer and enhance the strength of the NTA structure and conductivity of the inner layer.

The method proposed by the authors was used as a basis and several additional processing stages were added in order to obtain a template with the desired qualities.

Materials and methods

All chemicals were analytical reagent grade. Composites were obtained by the original method, which includes the stages of preliminary preparation of the titanium substrate [13], such as degreasing in NaOH and etching in 6 M HCl. The technical titanium grade was VT1-0. Next, the Ti substance grew enhanced TiO_2 nanotubes follows the twice anodization and cathodization process, as proposed in ref. [10], since the anodization technique is one of the well-known and straightforward methods, which provides a wide area of uniform nanotubes on Ti foil and enables the fine-tuning of the thickness of the film oxide layer [9], among other approaches. According to refs. [10,11], the structure strength of a NTA can be improved by a second anodization using a H_3PO_4/EG solution to form an additional compact layer, which can eliminate the fluoride-rich TiO_2 layer during the synthetic process. The above strategy enhances the attachment of the NTA to the Ti substrate. Additionally, the conductivity of NTAs is low but can be improved by cathodization for further combination with a coating layer [11]. Coatings were obtained on titanium foil with an area of 1 cm^2. The original TiO_2 nanotubes were prepared by anodizing Ti foil in ethylene glycol with 0.3 wt.% ammonium fluoride and 2 vol.% water at a constant potential for 3 h (1st anodization), followed by another anodizing in ethylene glycol with 5 wt.% H_3PO_4 (2nd anodization). The reduction was conducted in 1 M $HClO_4$ during 1 h (electrochemical reduction). Some samples were thermally treated in the air using tube furnace at 500°C for 3 hrs (thermal treatment).

Surface morphology was studied by scanning electron microscopy (SEM) with Tescan Vega 3 LMU with energy-dispersive X-ray microanalyzer Oxford Instruments Aztec ONE with X-Max^{N}20 detector. X-Ray powder diffraction (XRPD) data were collected in the transmission mode on a STOE STADI P diffractometer with Cu$K\alpha_1$-radiation, curved Ge (1 1 1) monochromator on primary beam, $2\theta/\omega$-scan, angular range for data collection of 20.000–110.225° (2θ) with increment of 0.015, linear position sensitive detector with step of recording of 0.480° (2θ), times per step of 75–300 s; U=40 kV, I=35 mA, and T=298 K. A calibration procedure was performed utilizing SRM 640b (Si) and SRM 676 (Al_2O_3) NIST standards. Preliminary data processing and X-ray qualitative phase analysis were performed using STOE WinXPOW and PowderCell program packages. Crystal structures of the phases were refined by the Rietveld method with the program FullProf.2k, applying a pseudo-Voigt profile function and isotropic approximation for the atomic displacement parameters, together with quantitative phase analysis.

Oxygen and hydrogen evolution reactions were investigated by steady-state polarization and by electrode impedance method on computer controlled GAMRY Potentiostat/Galvanostat/ZRA Reference 3000 in different electrolytes depending on the

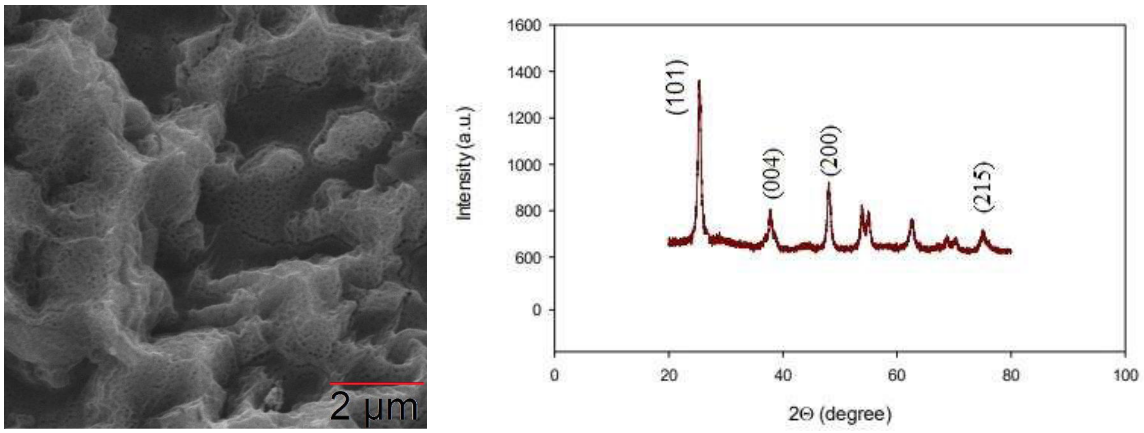

a b

Fig. 1. SEM image: planar view (a) and XPRD pattern (b) of film oxide layer obtained by two anodization and reduction steps

purposes of experiment.

Results and discussion

Study on surface morphology of the TiO_2 nanotubes revealed formation of nanotubes with an inner diameter in the range of 70–100 nm with a wall thickness of about 15–20 nm (Fig. 1,a). The surface morphology obtained by first anodization process demonstrates pattern of nanocombs having a diameter of about 130 nm. This nanocombed pattern acted as a template for the growth of much smaller diameter nanotubes during the second anodization in the mixture of ethylene glycol and phosphoric acid.

According to the EDX patterns, uniform distributions of elements in the NTA lattice (35.3% O and 51.5% Ti) were observed.

To confirm the existence of NTA in the hybrid nanomaterials, XRD experiments were employed for the structural analysis of obtained nanostructures (Fig. 1,b). XRD results illustrate that after annealing at 500^0C for 3 h, NTA are converted to anatase phases with a high degree of crystallinity. The diffraction peaks at $2\theta=25.3^0$, 37.8^0, 48.0^0, and 55.1^0 are attributed to the (101), (004), (200), and (211) anatase planes of NTA, respectively [10]. Phase composition of this film was TiO_2 anatase 57.6(9) wt.%; and Ti 42.4(5) wt.%.

If the surface region of the semiconductor electrode in the investigated potential range is depleted of majority carriers, the experimental data obtained by measuring the electrode capacitance should be linear in coordinates C^{-2} vs. E and follow the Mott-Schottky equation:

$$C^{-2} = \frac{2}{e\varepsilon\varepsilon_0 N}\left(E - E_{fb} - \frac{kT}{e}\right), \quad (1)$$

where C is the capacitance of the electrode; e is the electron charge; N is the carrier concentration; E_{fb} is the flat-band potential; k is the Boltzmann constant; T is the absolute temperature; ε is dielectric constant and ε_0 is the electric constant.

As previous studies have shown [13], MnO_2 and Ebonex® are highly doped semiconductors ($N>10^{18}$ cm^{-3}), so the Helmholtz layer capacitance C_H [8] needs to be taken into account in the Mott-Schottky equation:

$$C^{-2} = C_H^{-2} + \frac{2}{e\varepsilon\varepsilon_0 N}\left(E - E_{fb} - \frac{kT}{e}\right). \quad (2)$$

The slopes of equations (1) and (2) are equal, but unlike the value of E_{fb} obtained from (1):

$$E_{fb} = E_{C^{-2}=0} - \frac{kT}{e}, \quad (3)$$

in the second case, one has

$$E_{fb} = E_{C^{-2}=0} + \frac{e\varepsilon\varepsilon_0 N}{2C_H^2} - \frac{kT}{e}. \quad (4)$$

Impedance measurements were carried out in order to investigate the semiconducting properties of the samples involved. Solution of 1 M $HClO_4$ was used for impedance measurements to eliminate effects of adsorption. At a frequency of 1000 Hz, the C^{-2} vs. E dependences for investigated samples are linear over a wide range of potentials (Fig. 2). Carrier concentrations were found from the slopes of the lines, and flat-band potentials were determined from the segments cut off from the curves using equation (4). The results are presented in Table 1. The slope b in Table 1 is related to semiconductor material parameters such as band gap and electron mobility.

The line obtained for sample 3 (Fig. 3) is characterized by positive slope, indicating that the

Table 1

Semiconductor properties of TiO_2 nanotube arrays

No.	Synthesis conditions	b, V	N, cm^{-3}	E_{fb}, V
1	1st anodization; 2nd anodization	$1.31 \cdot 10^{10}$	$2.7 \cdot 10^{20}$	–2.7
2	1st anodization; 2nd anodization; thermal treatment	$1.3 \cdot 10^{10}$	$2.7 \cdot 10^{20}$	0.18
3	1st anodization; 2nd anodization; electrochemical reduction	$1.96 \cdot 10^{9}$	$1.8 \cdot 10^{21}$	–0.87
4	1st anodization; 2nd anodization; electrochemical reduction; thermal treatment	$5.02 \cdot 10^{9}$	$7.03 \cdot 10^{20}$	–0.02

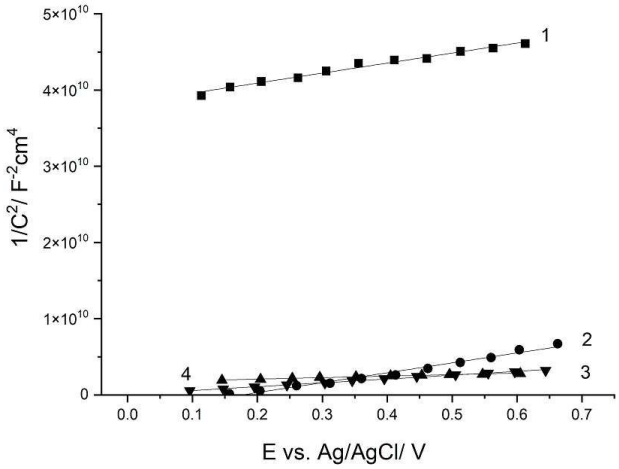

Fig. 2. Mott-Schottky plots for investigated samples. Synthesis conditions are shown in Table 1. Frequency is 1000 Hz

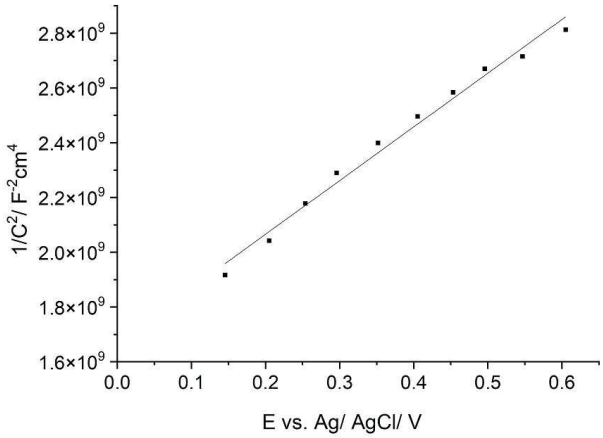

Fig. 3. Mott-Schottky plot for electrode obtained by twice anodization and cathodization process (sample 3). Frequency is 1000 Hz

studied material is an n-type semiconductor. Anodic polarization of such electrodes will lead to carrier depletion of the semiconductor above the flat-band potential. This, in turn, will lead to a decrease in the capacitance of the semiconductor component and an increase in the slope of the polarization curve plotted in semi-logarithmic coordinates [13].

The data presented in Figs. 2, 3 and Table 1 are in satisfactory agreement, as an increase in the flat-band potential leads to a decrease in the total potential and an increase in the number of carriers leads to a decrease in the slope of the polarization curve.

Heat treatment after the second and third stage, or the absence of the third stage of reduction in 1 M $NaClO_4$, leads to a decrease in the number of charge carriers (Table 1, Figs. 2 and 3).

Polarization curves represented in semilogarithmic scale for electrodes in 1 M $HClO_4$ (at a potential scan rate of 5 mV s^{-1}) are shown in Fig. 4. Oxygen overpotential depends on synthesis conditions. In all cases, E vs. lg j curves are linear and characterized by a high slope (>0.150 V dec^{-1}). It is well recognized that mechanism of the oxygen evolution reaction on oxide electrodes, TiO_2 in particular, in acidic media assumes that the rate-determining step is the first electron transfer, and the Tafel slope is 118 mV dec^{-1}. In this work, however, there is a distortion of the polarization curves, although the studies were carried out in an acidic solution, which did not contain specifically adsorbed ions. This denotes an increased semiconductive component or porosity effects (Table 2).

The slope of the resulting dependence will be determined by the semiconductor characteristics of the coating, which, in turn, will depend on the stoichiometry of the obtained oxide. The higher the stoichiometry in the oxygen sublattice, the lower the number of carriers, the charge number, and the contribution of the semiconductor component to the Tafel slope will be greater.

The coating obtained as a result of two anodizations consists mainly of unstable hydrated oxide with a large proportion of defects, and the contribution of the semiconductor component to the slope will be average. Thermal treatment promotes the conversion of part of the hydroxide into an oxide, but on the other hand, there is an additional increase in oxygen content (treatment in an oxygen atmosphere), and the flat band zone increases.

The reduction of nanotubes leads to a decrease in the number of hydrated areas and a decrease in the flat band zone, which affects the magnitude of

Table 2

Electrocatalytic activity in OER

No.	Synthesis conditions	Tafel slope, mV dec^{-1}
1	1st anodization; 2nd anodization	151
2	1st anodization; 2nd anodization; thermal treatment	169
3	1st anodization; 2nd anodization; electrochemical reduction	106
4	1st anodization; 2nd anodization; electrochemical reduction; thermal treatment	221

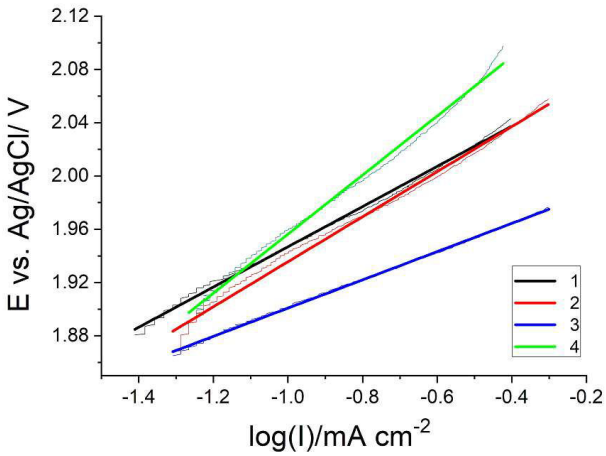

Fig. 4. Polarization curves of oxygen evolution reaction in 1 M $HClO_4$ represented in semilogarithmic scale. Potential scan rate 5 mV s^{-1}. Synthesis conditions are shown in Table 1.

the Tafel slope.

Introduction of lattice defects in TiO_2 can facilitate the creation of a new electronic band and expand its light absorption into the visible range [14]. Assuming that defects can be «planted» in anodized TiO_2 by oxygen-deficient anodization of Ti in a low-oxygen environment. The aim is to propose a new method for producing non-stoichiometric TiO_2 and achieve a breakthrough in visible light-driven TiO_2 photocatalysis.

It is generally accepted that the hydrogen evolution reaction (HER) can occur via two possible mechanisms in an acidic environment [8]. The reaction starts with hydrogen electrochemical adsorption on the catalyst surface, which is known as the Volmer reaction (5). This involves the transfer of one electron to form an intermediate adsorbed hydrogen atom [8]:

$$H^+_{(aq)}+e^-\rightarrow H_{ads} \text{ (Volmer)} \quad (5)$$

The next step involves the formation of hydrogen molecules through two alternative routes: the adsorbed species can react with a proton from the electrolyte in the Heyrovsky reaction (6) or it can combine with other adsorbed hydrogen atoms on the catalyst surface to generate H_2 via the Tafel reaction (7):

$$H^+_{(aq)}+H_{ads}+e^-\rightarrow H_{2(g)} \text{ (Heyrovsky)} \quad (6)$$

$$H_{ads}+H_{ads}\rightarrow H_{2(g)} \text{ (Tafel)} \quad (7)$$

The actual HER mechanism for a given catalyst can be analyzed in terms of the Tafel slope, which is the slope of potential vs. logarithm of current density profiles. These values can be determined by theoretical kinetic analysis of the HER in acid media, as follows [15]: (i) if the Heyrovsky and Tafel reactions are much faster than the Volmer step, theoretical calculations would predict a Tafel slope of 0.118 V dec^{-1} at 25°C; (ii) if the mechanism is assumed to be formed only by the Volmer/Heyrovsky reactions, with the Heyrovsky reaction being the rate-determining step, the theoretical Tafel slope would result in 0.040 V dec^{-1}; (iii) finally, if the mechanism is formed by the Volmer/Tafel steps, having the Tafel reaction as the limiting step, the theoretical slope results in 0.030 V dec^{-1}.

Polarization curves on hydrogen evolution in acidic medium are presented in Fig. 5. The calculated Tafel slopes of the materials involved are summarized in Table 3. All the layers are characterized by a high Tafel slope. The layers obtained after heat treatment (3 and 4) are characterized by a lower Tafel slope (175 mV dec^{-1}).

Under cathodic polarization of electrodes in an acidic solution at low current densities, the proton donor is the hydroxonium ion. The rate-determining step of the hydrogen evolution process depends on the treatment of the material. As the electrode potential shifts towards the cathode and the cathodic current density increases, diffusion limitations arise. Then, the limiting current for hydroxonium ions is reached, and in the vicinity of active centers where H_3O^+ ions are discharged, local alkalization of the electrolyte occurs, creating conditions for the formation of titanium hydroxide hydrosol, which has the ability to firmly adsorb on various surfaces. An increase in the fraction of the electrode surface covered with $TiO(OH)_2$ and an increase in the

Table 3

Electrocatalytic activity in HER

No.	Synthesis conditions	Tafel slope, mV dec^{-1}
1	1st anodization; 2nd anodization	218
2	1st anodization; 2nd anodization; thermal treatment	294
3	1st anodization; 2nd anodization; electrochemical reduction	173
4	1st anodization; 2nd anodization; electrochemical reduction; thermal treatment	175

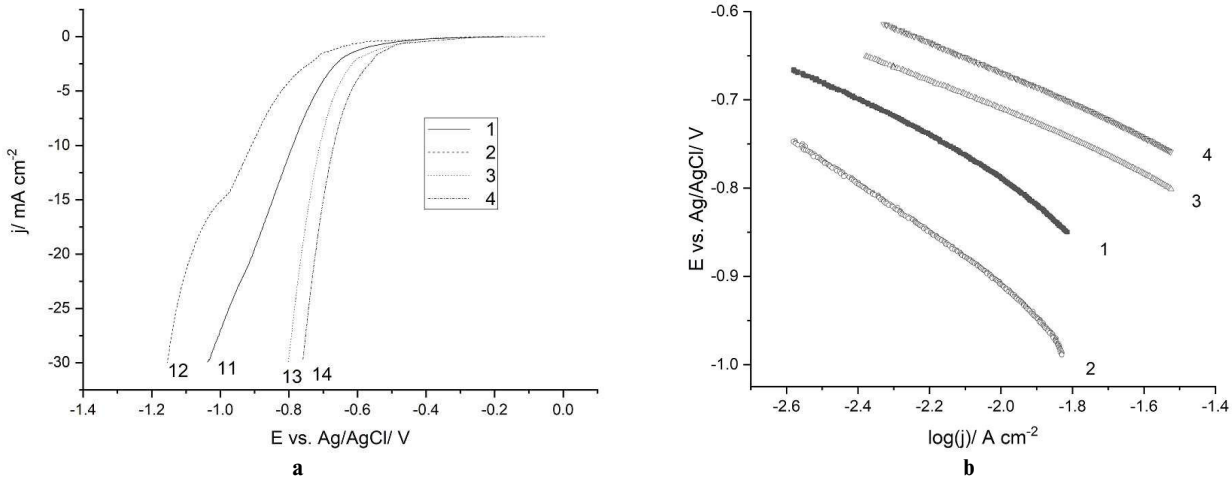

Fig. 5. Polarization curves of hydrogen evolution reaction obtained in 1 M $HClO_4$ (a); comparison of Tafel plots for samples (b). Potential scan rate 5 mV s^{-1}. Synthesis conditions zre shown in Table 1

thickness of the hydrated titanium hydroxide film over time lead to a slight decrease in the rate of hydrogen evolution, which is observed when registering potentiodynamic polarization curves at negative potentials above −1000 mV. The decrease in current is particularly noticeable at higher potential scan rates. At the limiting current area, the rate of the process is limited by the diffusion of H_3O^+ ions through the thin colloidal film of titanium hydroxide and does not depend on mixing.

The studied system is non-stoichiometric. It is not only structurally but also chemically heterogeneous, as there are areas on the surface containing titanium oxide or hydroxide. Two processes occur in the system: (i) hydrogen evolution, and (ii) proton diffusion, which leads to the reduction of the oxide. Although it accumulates in the bulk, it changes the composition of the coating surface.

This means that heating the composites under the proposed conditions leads to enhancement in the HER kinetics as compared to the initial material. Moreover, the deposit phase composition also influences the HER. The increase in electrochemical activity of titanium oxide layers may be related to the presence of nonstoichiometric Ti oxides. Creation of new active centers on the electrode surface influences the activity more than the simple effect of surface area increase.

Hydroxylated TiO_2 is a low-conducting material with a small number of active centers. The Tafel slope increases as one can see in Table 3. When one conducts thermal treatment, the proportion of stoichiometric TiO_2 increases, and when one reduces the material, it partially restores the oxide, forming hydroxylated TiO_2 and possibly titanium suboxides. In the oxygen sublattice, oxygen is replaced by OH^- ions, and the width of the bandgap decreases. One then further stabilizes the surface, removes the non-conducting hydroxylated portion, and the system on the surface becomes more crystalline, making it more conductive. One observe a decrease in hydrogen evolution overpotential on materials that undergo only two stages of anodic treatment, and the reduction processes on such a material, including metal deposition, are inhibited, while on materials that undergo all stages of treatment, the phase is sufficiently stable. These materials work more on the principle of titanium suboxides like Ebonex®.

If the target process when using the coating is not hydrogen evolution, but for example, cathodic dehydrohalogenation of organic substances, then it is necessary for the hydrogen evolution overpotential to be high. If the process occurs with diffusive kinetics, then hydrogen will be released later, and

the target process (dehydrohalogenation) will proceed with a higher current efficiency, and a drop in this current efficiency will occur later.

Having in mind the above mentioned the system involved is of interest as (i) a template for the subsequent creation of photo- and electrocatalysts by electrochemical deposition of metals, which will act as electron donors; (ii) cathode material in dehydrohalogenation reactions; and (iii) anode material in electroplating, since when using this type of coating the components of the electrolyte do not oxidize, as was shown in ref. [13].

Conclusions

The investigated material, as a non-stoichiometric semiconductor, is of certain interest as a substrate for creating photo- and electrocatalysts. High overvoltage of hydrogen evolution widens the range of possibilities for using this material for the reduction of organic compounds in aqueous solutions. The Tafel slope in OER for obtained materials is determined by the semiconductor characteristics of the coating, which, in turn, depended on the stoichiometry of the synthesized oxide. The higher the stoichiometry in the oxygen sublattice, the lower the number of carriers, the charge number, and higher the contribution of the semiconductor component to the Tafel slope. As for hydrogen evolution, the layers obtained after heat treatment are characterized by a lower Tafel slope (175 mV dec^{-1}).

Funding

This work was supported by Ministry of Education and Science of Ukraine (grant numbers 0122U001134; and 0123101809).

REFERENCES

1. *Development* of electrodeposited multilayer coatings: a review of fabrication, microstructure, properties and applications / Aliofkhazraei M., Walsh F.C., Zangari G., et al. // Appl. Surf. Sci. Adv. – 2021. – Vol.6. – Art. No. 100141.

2. *Walsh F.C.* Modern developments in electrodes for electrochemical technology and the role of surface finishing // Trans. Inst. Met. Finish. – 2019. – Vol.97. – No. 1. – P.28-42.

3. *The use* of anodic oxides in practical and sustainable devices for energy conversion and storage / Santos J.S., Araujo P.d.S., Pissolitto Y.B., et al. // Materials. – 2021. –Vol.14. – P.383-421.

4. *Martinez-Huitle C.A., Ferro S.* Electrochemical oxidation of organic pollutants for the wastewater treatment: direct and indirect processes // Chem. Soc. Rev. – 2006. –Vol.35. – P.1324-1340.

5. *Panizza M. Cerisola G.* Direct and mediated anodic oxidation of organic pollutants // Chem. Rev. – 2009. – Vol.109. – P.6541-6569.

6. *Shmychkova O., Girenko D., Velichenko A.* Noble metals doped tin dioxide for sodium hypochlorite synthesis from low concentrated NaCl solutions // J. Chem. Technol. Biotechnol. – 2022. – Vol.97. – No. 4. – P.903-913.

7. *Material* selection and optimization of conditions for electrooxidation of nitrofurazone: a comparative study of tin and lead dioxides / Shmychkova O., Zahorulko S., Girenko D., et al. // J. Electrochem. Soc. – 2021. – Vol.168. – No. 8. – Art. No. 086507.

8. *Effects* of metal–support interaction in the electrocatalysis of the hydrogen evolution reaction of the metal-decorated titanium dioxide supported carbon / Ometto F.B., Paganin V.A., Hammer P., et al. // Catalysts. – 2023. – Vol.13. – P.22-37.

9. *Sugiawati V.A., Vacandio F., Djenizian Th.* All-solid-state lithium ion batteries using self-organized TiO_2 nanotubes grown from Ti-6Al-4V alloy // Molecules. – 2020. – Vol.25. – P.2121-2136.

10. *Electrochemical* oxidation of reverse osmosis concentrates using enhanced TiO_2-NTA/SnO_2-Sb anodes with/without PbO_2 layer / Chen M., Pan Sh., Zhang C., et al. // Chem. Eng. J. – 2020. – Vol.399. – Art. No. 125756.

11. *Kinetic*, mechanism and mass transfer impact on electrochemical oxidation of MIT using Ti-enhanced nanotube arrays/SnO_2-Sb anode / Chen M., Wang C., Wang Y., et al. // Electrochim. Acta. – 2019. – Vol.323. – Art. No. 134779.

12. *High-performance* and renewable supercapacitors based on TiO_2 nanotube array electrodes treated by an electrochemical doping approach / Wu H., Li D.D., Zhu X.F., et al. // Electrochim. Acta. – 2014. – Vol.116. – P.129-136.

13. *Electrochemical* properties of thermally treated platinized Ebonex® with low content of Pt / Kasian O.I., Luk'yanenko T.V., Demchenko P.Yu., et al. // Electrochim. Acta. – 2013. – Vol.109. – P.630-637.

14. *Defective* TiO_2 with oxygen vacancies: synthesis, properties and photocatalytic applications / Pan X., Yang M.Q., Fu X., et al. // Nanoscale. – 2013. – Vol.5. – P.3601-3614.

15. *Koutecky-Levich* analysis applied to nanoparticle modified rotating disk electrodes: Electrocatalysis or misinterpretation? / Masa J., Batchelor-Mcauley C., Schuhmann W., et al. // Nano Res. – 2014. – Vol.7. – P.71-78.

Received 07.03.2023

СИНТЕЗ МАТРИЦІ ДЛЯ СТВОРЕННЯ ФОТО- ТА ЕЛЕКТРОКАТАЛІЗАТОРІВ

В. Книш, О. Шмичкова, Т. Лук'яненко, О. Величенко

В цій роботі підібрані оптимальні умови синтезу матриці для створення фото- та електрокаталізаторів. Зокрема, показано, що TiO_2 нанотрубки мають високу питому поверхню і покращені каталітичні властивості, але мають низьку провідність і слабку міцність конструкції, що потребує подальшої оптимізації. Вихідні нанотрубки TiO_2 були синтезовані шляхом анодування Ti фольги в етиленгліколі з 0,3 мас.% амонію фториду та 2 об.% води при постійному потенціалі з

наступним анодуванням в етиленгліколі з 5 мас.% H_3PO_4. Відновлення проводили в 1 М $HClO_4$. Частина зразків була термічно оброблена на повітрі в трубчастій печі. Показано, як умови синтезу покриття впливають на морфологію та стехіометрію одержуваного оксидного покриття. Для одержаних матеріалів нахил Тафеля в реакції виділення кисню визначається напівпровідниковими характеристиками покриття, які, в свою чергу, залежать від стехіометрії синтезованого оксиду. Чим вища стехіометрія в кисневій підрешітці, тим менше носіїв заряду і тим більший внесок напівпровідникового компонента в нахил Тафеля. Що стосується виділення водню, то покриття, одержані після термічного оброблення, характеризуються меншим нахилом Тафеля (175 мВ).

Ключові слова: масиви титаноксидних нанотрубок; внутрійшній шар; напівпровідникові властивості; електроосадження, реакція виділення кисню; реакція виділення водню.

TEMPLATE SYNTHESIS FOR THE CREATION OF PHOTO- AND ELECTROCATALYSTS

V. Knysh, O. Shmychkova, T. Luk'yanenko, A. Velichenko *

Ukrainian State University of Chemical Technology, Dnipro, Ukraine

* **e-mail: velichenko@ukr.net**

This work reports the optimal conditions for the synthesis of a matrix for the creation of photo- and electrocatalysts. Specifically, it is shown that TiO_2 nanotube arrays has a high specific surface area and improved catalytic properties, but has low conductivity and weak structural strength, that requires further optimization. The original TiO_2 nanotubes were prepared by anodizing of Ti foil in ethylene glycol with 0.3 wt.% ammonium fluoride and 2 vol.% water at a constant potential, followed by another anodizing in ethylene glycol with 5 wt.% H_3PO_4. The reduction was conducted in 1 M $HClO_4$. Some samples were thermally treated in the air using tube furnace. The study demonstrates how the synthesis conditions of the coating affect the morphology and stoichiometry of the resulting oxide coating. For the obtained materials, the Tafel slope in the oxygen evolution reaction is determined by the semiconductor characteristics of the coating, which, in turn, depend on the stoichiometry of the synthesized oxide. The higher the stoichiometry in the oxygen sublattice, the fewer the charge carriers and the greater the contribution of the semiconductor component to the Tafel slope. As for hydrogen evolution, the layers obtained after heat treatment show a lower Tafel slope (175 mV dec^{-1}).

Keywords: titanium nanotube arrays; inner layer; semiconductor properties; electrodeposition; oxygen evolution reaction; hydrogen evolution reaction.

REFERENCES

1. Aliofkhazraei M, Walsh FC, Zangari G, Kockar H, Alper M, Rizal C, et al. Development of electrodeposited multilayer coatings: a review of fabrication, microstructure, properties and applications. *Appl Surf Sci Adv*. 2021; 6: 100141. doi: 10.1016/j.apsadv.2021.100141.

2. Walsh FC. Modern developments in electrodes for electrochemical technology and the role of surface finishing. *Trans Inst Met Finish*. 2019; 97: 28-42. doi: 10.1080/00202967.2019.1551277.

3. Santos JS, dos Santos Araujo P, Pissolitto YB, Lopes PP, Simon AP, de Souza Sikora M, et al. The use of anodic oxides in practical and sustainable devices for energy conversion and storage. *Materials*. 2021; 14: 383. doi: 10.3390/ma14020383.

4. Martinez-Huitle CA, Ferro S. Electrochemical oxidation of organic pollutants for the wastewater treatment: direct and indirect processes. *Chem Soc Rev*. 2006; 35: 1324-1340. doi: 10.1039/B517632H.

5. Panizza M, Cerisola G. Direct and mediated anodic oxidation of organic pollutants. *Chem Rev*. 2009; 109: 6541-6569. doi: 10.1021/cr9001319.

6. Shmychkova O, Girenko D, Velichenko A. Noble metals doped tin dioxide for sodium hypochlorite synthesis from low concentrated NaCl solutions. *J Chem Technol Biotechnol*. 2022; 97: 903-913. doi: 10.1002/jctb.6973.

7. Shmychkova O, Zahorulko S, Girenko D, Luk'yanenko T, Dmitrikova L, Velichenko A. Material selection and optimization of conditions for electrooxidation of nitrofurazone: a comparative study of tin and lead dioxides. *J Electrochem Soc*. 2021; 168(8): 086507. doi: 10.1149/1945-7111/ac1e58.

8. Ometto FB, Paganin VA, Hammer P, Ticianelli EA. Effects of metal−support interaction in the electrocatalysis of the hydrogen evolution reaction of the metal-decorated titanium dioxide supported carbon. *Catalysts*. 2023; 13: 22. doi: 10.3390/catal13010022.

9. Sugiawati VA, Vacandio F, Djenizian T. All-solid-state lithium ion batteries using self-organized TiO_2 nanotubes grown from Ti-6Al-4V alloy. *Molecules*. 2020; 25: 2121. doi: 10.3390/molecules25092121.

10. Chen M, Pan S, Zhang C, Wang C, Zhang W, Chen Z, et al. Electrochemical oxidation of reverse osmosis concentrates using enhanced TiO_2-NTA/SnO_2-Sb anodes with/without PbO_2 layer. *Chem Eng J*. 2020; 399: 125756. doi: 10.1016/j.cej.2020.125756.

11. Chen M, Wang C, Wang Y, Meng X, Chen Z, Zhang W, et al. Kinetic, mechanism and mass transfer impact on electrochemical oxidation of MIT using Ti-enhanced nanotube arrays/SnO_2-Sb anode. *Electrochim Acta*. 2019; 323: 134779. doi: 10.1016/j.electacta.2019.134779.

12. Wu H, Li D, Zhu X, Yang C, Liu D, Chen X, et al. High-performance and renewable supercapacitors based on TiO_2 nanotube array electrodes treated by an electrochemical doping approach. *Electrochim Acta*. 2014; 116: 129-136. doi: 10.1016/j.electacta.2013.10.092.

13. Kasian OI, Luk'yanenko TV, Demchenko P, Gladyshevskii RE, Amadelli R, Velichenko AB. Electrochemical properties of thermally treated platinized Ebonex® with low content of Pt. *Electrochim Acta*. 2013; 109: 630-637. doi: 10.1016/j.electacta.2013.07.162.

14. Pan X, Yang MQ, Fu X, Zhang N., Xu YJ. Defective TiO_2 with oxygen vacancies: synthesis, properties and photocatalytic applications. *Nanoscale*. 2013; 5: 3601-3614. doi: 10.1039/C3NR00476G.

15. Masa J, Batchelor-Mcauley C, Schuhmann W, Compton RG. Koutecky-Levich analysis applied to nanoparticle modified rotating disk electrodes: electrocatalysis or misinterpretation? *Nano Res*. 2014; 7: 71-78. doi: 10.1007/s12274-013-0372-0.